Full-waveform Inversion workflow for evaluating sparse-node survey design in deep water Santos Basin

Yannick Cobo, Rodrigo Felicio Fuck, Carlos Calderon, Chao Wang and Paul Farmer, ION Geophysical

Abstract

We carry out a series of experiments on an OBN dataset for understanding the effect of decimating sources and receivers for velocity estimation with a Full Waveform Inversion (FWI) workflow that minimizes cycle skipping. The experiments are performed in synthetic as well as field datasets from an OBN survey shot over complex geology from a pre-salt play in Santos Basin, Brazil. The automated FWI workflow facilitates studying the data decimation influence on the inversion outcomes. Results show that sparser datasets produce velocity models that loose accuracy and resolution in comparison to a denser base geometry. Nevertheless, these models (from sparser versions of the same dataset) are still able to delineate the geometry of salt geobodies and minibasins. In particular, OBN surveys with a 1 km by 1 km node spacing with a carpet of sources sampled at 100 m by 300 m are indeed a viable alternative to denser (and more expensive) OBN surveys acquired with a 500 m by 500 m node sampling and a shot carpet of 50 m by 50 m.

Introduction

With the realization that FWI from long offsets and low frequencies, there is a recent trend in seismic exploration towards the use of Ocean Bottom Nodes (OBNs) for the specific purpose of estimating more accurate velocity models in complex geological settings. OBN data are being acquired with longer offsets and improved azimuth coverage than typical streamer surveys. To decrease the cost of OBN acquisition it is important to evaluate the effect of shot and receiver sampling for model building and imaging. We investigate how shot and receiver sampling affect the velocity model building primarily from long offsets by decimating a denser sampled baseline survey. We employ an automated FWI algorithm and workflow in synthetic and real seismic datasets. We asses the quality of the estimated models by comparing prestack field and synthetic data match QCs, model QCs, migrated gathers and stacks output by RTM and by Kirchhoff PSDM.

Method

We use field and acoustic-finite-difference synthetics derived data from an OBN survey shot in the Santos Basin, offshore Brazil. The study area is in ultradeep water (2 km) and the Geology is characterized of a 2 to 4 km thick sequence of mostly clastic sedimentary rocks overlaying evaporite layers and thick salt — mostly halite, with subordinate intervals of anhydrite, gypsum, tachyhydrite and carnalite. These salt layers have a complex structural history and may form massive heterogeneous bodies of up to 3 km of thickness, displaying a complex array of folds, faulting, overhangs and minibasins. Below these units the presalt is comprised of syn-rift sequences of clastic sediments, basalts, carbonates and evaporites, which include reservoir rocks (Carlotto et al., 2017).

The OBN survey contains about 3000 nodes deployed on a 500 m by 500 m regular spacing grid, while the shots were acquired on a 50 m by 50 m shot carpet grid, yielding rich azimuth data coverage with offsets as large as 27 km (see Figure 1).

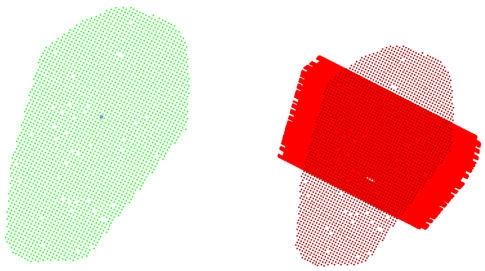

(a) (b)

Figure 1: (a) node layout and (b) one node shot carpet. Node spacing of 500 m x 500 m, shot spacing of 50 m x 50 m. Maximum offset is about 27 km

To evaluate the effect of sparser geometries for velocity estimation from long offsets, we consider a number of shot and receiver decimation scenarios from the original survey. The datasets are used as input to a velocity model building FWI workflow, with similar method parameterizations for each of the tests. All tests use the same starting initial velocity model and the same data-derived source wavelet. Pre-processing of the input field data comprised debubble filtering, source deghosting and zero phasing of the hydrophone data.

The prposed FWI workflow is a cascaded flow that uses two disctictive cost functions that emphasize traveltime differences to minimize cycle skipping (Wang et al., 2019). The first step uses picked first-break events that are matched with the syntehtic data. We call this step first-arrival FWI or FA-FWI, an approach akin to that of Sheng et al. (2006). Once FA-FWI converges to a solution for ultralow to low frequencies (< 4 Hz), we use travel-time FWI (TTFWI), which matches waveforms of diving waves and wide-angle reflections on relatively short time windows

referenced to the picked first arrival.

Both FA- and TT-FWI use a hierarchical scheme in frequency, starting from the lowest frequencies in the data (< 3 Hz) and progressing up to 5.5 Hz, at intervals of 0.5 Hz, designed to gradually build the velocity model from low to high wavenumbers (e.g. Virieux and Operto, 2009). The data mutes select diving wave energy starting at around 6 km offset, with data windows for TT-FWI being gradually modified to include more events as the iterations progress. The offset range inverted prevents incorporating direct arrivals into the process. A key aspect in our workfow is that high contrast layers are not part of the starting model and are hence built by FWI.

Results

We first illustrate how decimating receivers affects the FWI inverted model by comparing the results obtained for two 3D synthetic datasets, which differ only by having shot carpets that are 100 m by 100 m in one case and 100 m by 300 m in the other, corresponding to decimation of shot lines from the base acquisition. The geometry for the synthetic datasets has been taken from the actual field data, while the "true velocity" model is a high-grade velocity model derived from running FWI for a bandwidth of 2 to 10 Hz, in addition to iterations of reflection tomography guided also by interpretation of top of salt and depth control from well information.

Figure 2 compares the depth slices of the two models derived from the synthetic datasets and that of the "true velocity". Both models converge to very similar results starting from the same initial smooth velocity model, delineating the salt bodies (green colors in the reference "true velocity" model) and the sedimentary minibasins. A close inspection of these results, Figures 2a and 2b, reveal that the model derived from the denser shot carpet provides a more accurate match with the true velocity, with a higher resololution of boundaries for the salt and the minibasins. In addition, the models with sparser shot carpets also experienced slower convergence and localized cycle-skipping. Overall, the two models produce depth RTM images of comparable quality, but the denser shot sampling produces flatter gathers, a simpler base of salt and better focused images of the pre-salt sequence, highlighted by the arrows shown in Figures 3a and 3b. We note that the stacks were derived from the migration of the actual OBN field data, but using the models derived from synthetic datasets, similar to the work of Mei et al. (2019).

Next we test four different scenarios, all of which use the FWI workflow as in the previous tests, but now applied to the actual field OBN data. In the first test, we use the original geometry of the OBN survey, i.e., nodes distributed on 500 m by 500 m grid and shots on a 50 m by 50 m carpet; in the second, nodes are decimated to a 1 km by 1 km grid, while the shots are in a 100 m by 300 m carpet; in the third, nodes are further decimated to a 2 km by 2 km grid, whereas the shots are kept on the same 100 m by 300 m configuration; in the fourth, all nodes are used, but shots are decimated to 50 m by 200 m with maximum offset of 1 km across shotlines, such that a narrow-azimuth survey is emulated (we call this a "NAZ-like" scenario).

Comparisons of vertical sections of the FWI velocity models for the first three scenarios with the high-grade

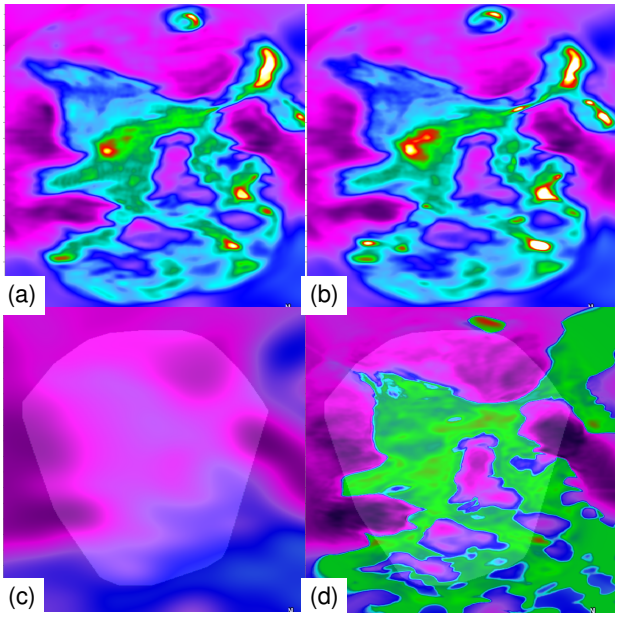

Figure 2: Depth slices for the models estimated by FWI for synthetic datasets with shot-carpets of (a) 100 m by 100 m and (b) 100 m by 300 m; (c) initial velocity model; (d) true velocity model.

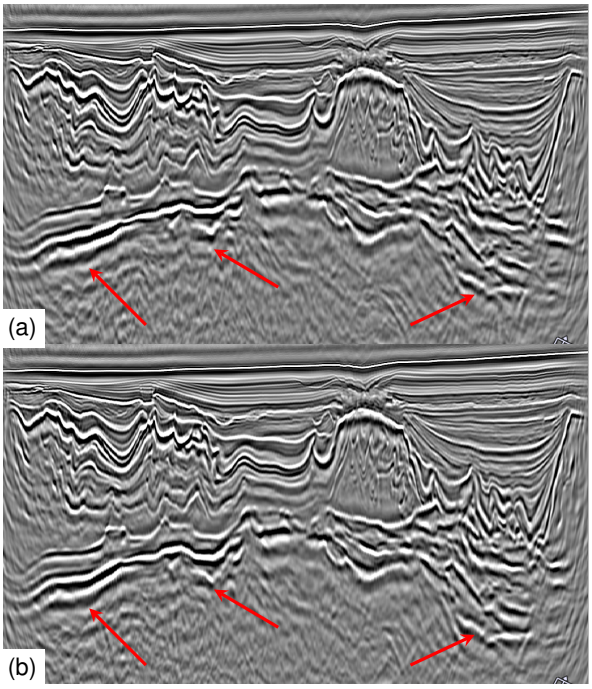

Figure 3: Vertical sections from 20Hz RTM stack volumes derived by migrating actual field data, using the model derived from synthetic data with (a) 100 m by 100 m and (b) 100 m by 300 m shot carpets.

model (Figure 4) show that all three reached similar solutions that recovered the bulk of the salt geometry from the initial model with no salt. The comparisons also reveal a gradual loss of model resolution as the nodes become sparser. As the node spacing increases, the FWI

workflow recovers smoother velocity gradients at the top of the salt; moreover, FWI introduces velocity oscillations in both the salt and presalt sections for the sparser node configurations. We highlight, however, that decimation of the nodes from 500 m to 1 km grids yields models of comparable quality, whereas decimations of 2 km lead to "noisier" solutions that require a more aggressive model regularization. Note also that the NAZ-like case—with dense nodes, but with azimuth distribution curtailed by the narrower shot carpets—produces the poorest solution of all. Not only the velocity gradients are smoother, but the sediment/salt interface is particularly ill-defined and lacks resolution such as the overhang feauture at the center of Figure 4e.

These observations are further corroborated by the inspection of depth slices presented in Figure 5 for all the four scenarios. Delineation of the salt bodies (velocities of about 4500 m/s, i.e., reddish to white colors) and of the minibasins compares well with the high grade model, but degrades as nodes become sparser. Likewise, the effect of reducing azimuth outweighs node decimation, imprinting a horizontal stripping parallel to the shotlines on the solution for the "NAZ-like" acquisition, significantly reducing the resolution of the salt bodies and the minibasins in comparison with all the other scenarios. Overall, the model derived from 1 km node spacing with rich azimuth coverage provides a good compromise in relation to the 500 m by 500 m base node spacing one, with oscillations in the estimated velocities and salt delineation not being as conspicuous as those seen in the model computed with the 2 km node spacing dataset.

The deleterious effect on model estimation caused by drastic reduction of azimuth sampling (i.e., long offsets are restricted to the shotline azimuth) can be better understood by comparing migrated images. Examination of Kirchhoff PSDM stacks (using legacy narrow-azimuth data available for the study area) displayed in Figure 6 show that model derived from the NAZ-like acquisition provides images with weak and discontinuous reflectors for the BoS and presalt events throughout the whole section. In addition, ToS is distorted, especially for the geobody at the center of the image in Figure 6d. In contrast, the model derived with 2 km by 2 km nodes (and with a sparser shot carpet), Figure 6c, clearly images these events, producing a stack that better approximate the stacks obtained from migration using either the production (Figure 6a) or the 500 m by 500 m nodes (Figure 6b) models in comparison to the image from the NAZ-like acquistion.

We further assess the loss of model resolution due to decimation by comparing the depth images from the first three scenarios models. Figure 7 displays a vertical section of stacks obtained from Kirchhoff PSDM (maximum frequency at 45 Hz) of OBN data without decimation. (Thus, in Figure 7, we compare only the effect of the data decimation on the velocity estimation, not on the imaging itself.) The progressive deterioration of salt bodies and minibasin delineation in the models from sparser nodes is reflected in their respective images as a gradual push-down of the ToS events, as the velocity gradients loose model resolution. Likewise, one notes a decrease in focusing and continuity of events marking the base of salt and pre-salt section, particularly beneath the minibasin on the right side of the sections. Despite the decrease in quality of the final image, Figure 7 reinforces the point that 1 km node spacing is able to produce models that allow imaging in comparable terms to a model derived from a 500 m node spacing survey.

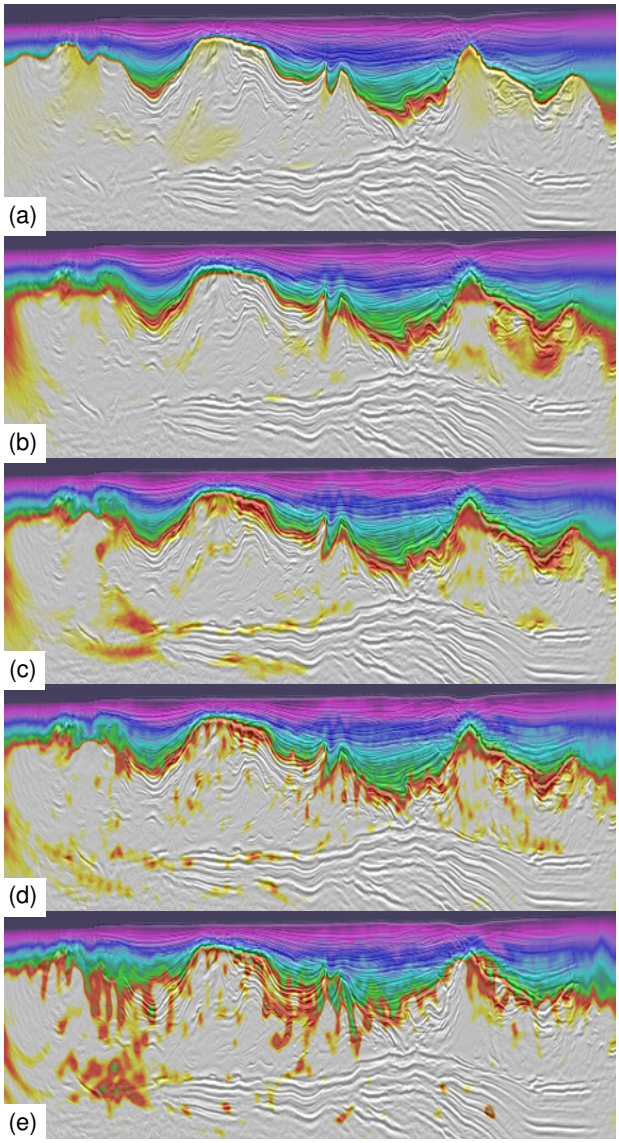

Figure 4: Vertical sections: (a) production velocity model, and FWI models using node grids of (b) 500 m by 500 m, (c) 1 km by 1 km and (d) 2 km by 2 km; (e) NAZ-like with 50 m by 200 m shot carpet. The stack from the production model is overlaid for reference in all plots.

Conclusions

The results presented lead to two main conclusions, which are applicable to velocity model estimations done using FWI from mostly diving wave energy and without imposing model priors. First, that poor azimuthal coverage is more detrimental to model estimation than node sparsity in a complex geology setting such as the one studied here. Second, that a sparse node geometry in general produces poorer velocity models than a relatively denser counterpart. These are true regardless of the frequency bandwidth at which the velocity is estimated, since FWI is a

non-linear problem that combines input signal frequencies and scattering angles (i.e., source-receiver geometry) to resolve model wavenumbers.

Nevertheless, coarser source-receiver distributions are still able to produce good approximations to the overall subsurface velocity model, provided that cycle skipping is avoided due to good SNR at low-frequencies in the data and to the use of traveltime-based cost functions such as those from FA- and TT-FWI. In our particular case (i.e., an OBN survey in ultradeep water and a complex geology setting) we find that a 1 km by 1 km grid of nodes with 100 m by 300 m shot-carpets are a viable alternative to denser node surveys with 4 times more nodes and 6 times more shots when velocity estimation is considered for data with large offsets, full azimuth coverage and low frequencies.

Acknowledgements

We thank ION and the consortium of partners Petrobras, Total, Shell Brasil, CNPC and CNOOC for permission to publish these results.

References

Carlotto, M. A., R. C. B. da Silva, A. A. Yamato, W. L. Trindade, J. L. P. Moreira, R. A. R. Fernandes, O. J. S. Ribeiro, W. Peres Gouveia, Jr., J. P. Carminati, D. Qicai, Z. Junfeng, and A. C. da Silva-Telles, Jr., 2017, Libra: A newborn giant in the Brazilian presalt province, *in* Giant Fields of the Decade 2000–2010:AAPG memoir 113: AAPG.

Mei, J., Z. Zhang, F. Lin, R. Huang, P. Wang, and C. Mifflin, 2019, Sparse nodes for velocity: Learnings from Atlantis OBN full-waveform inversion test: 89th Annual International Meeting, SEG, Expanded Abstracts, 167–171.

Sheng, J., A. Leeds, M. Buddensiek, and G. T. Schuster, 2006, Early arrival waveform tomography on near-surface refraction data: Geophysics, **71**, U47–U57.

Virieux, J., and S. Operto, 2009, An overview of full waveform inversion in exploration geophysics: Geophysics, **74**, WCC1–WCC26.

Wang, C., P. Farmer, T. Burley, C. Calderon, I. Jones, and J. Brittan, 2019, Preconditioned reflection full waveform inversion for subsalt imaging: 89th Annual International Meeting, SEG, Expanded Abstracts, 1214–1218.

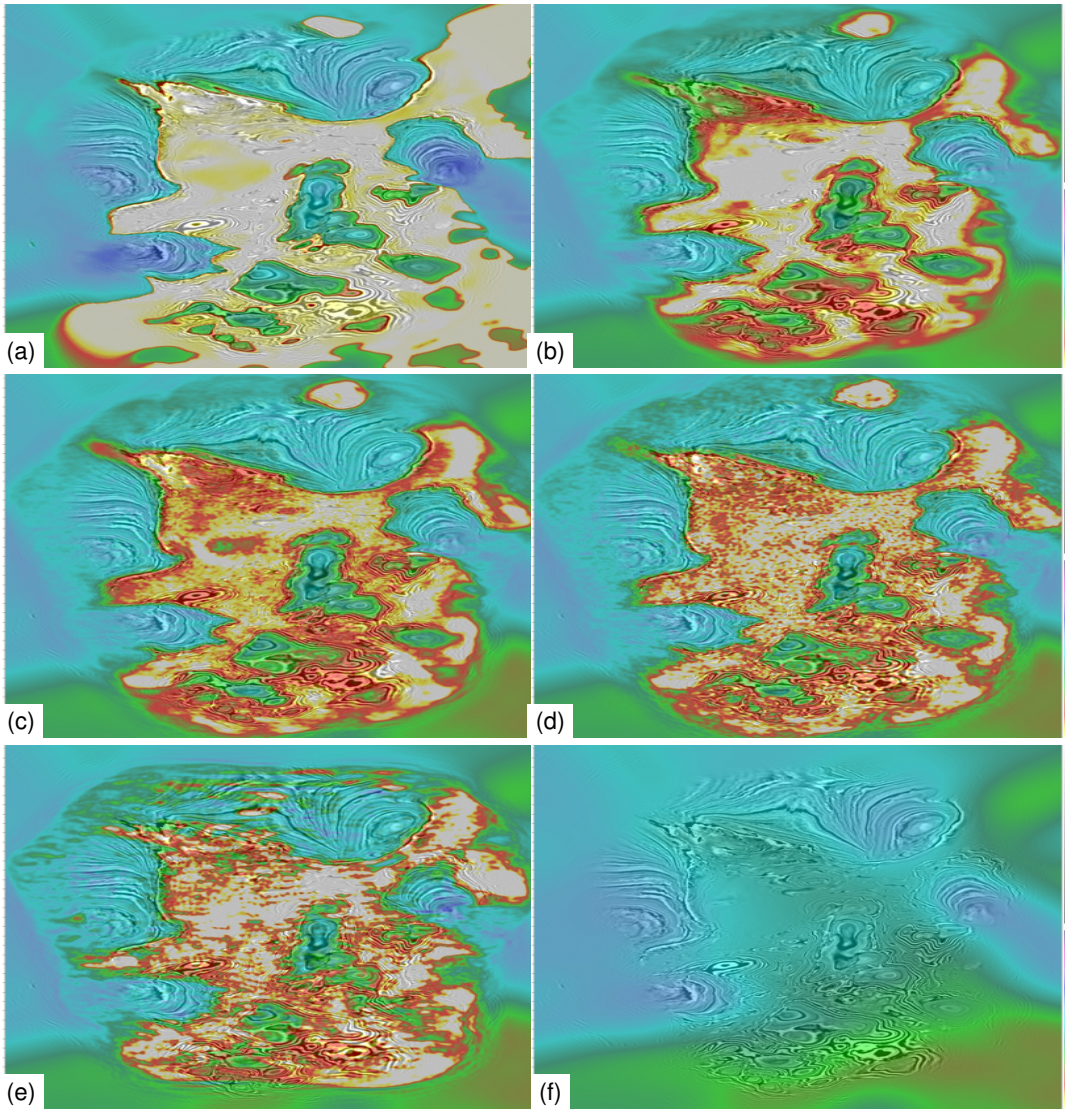

Figure 5: Depth slices for (a) production model and FWI-derived models with node grids of (b) 500 m by 500 m, (c) 1 km by 1 km, and (d) 2 km by 2 km. (e) NAZ-like survey with 50 m by 200 m shot carpets; (f) initial velocity model. The stack from the production model is overlaid for reference in all plots.

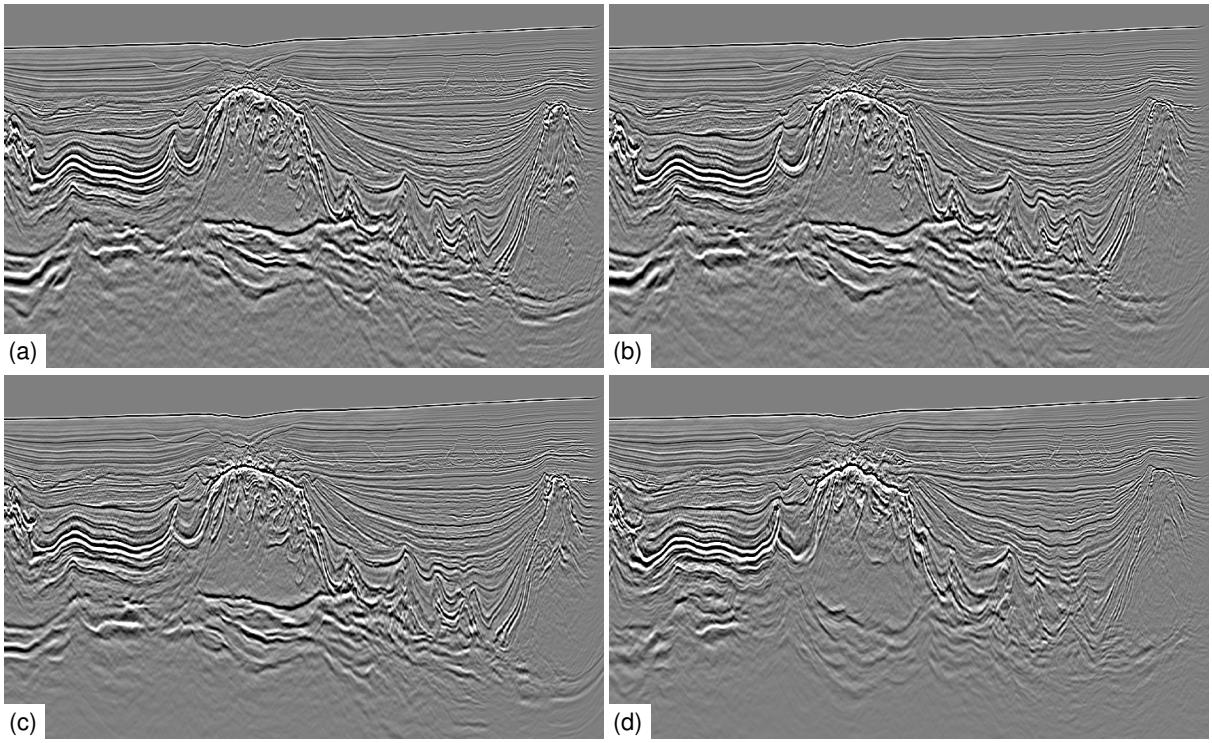

Figure 6: Kirchhoff PSDM stacks for legacy Narrow-azimuth data migrated with (a) production model and the FWI-derived models with node grids of (b) 500 m by 500 m, (c) 2 km by 2 km, and (d) NAZ-like.

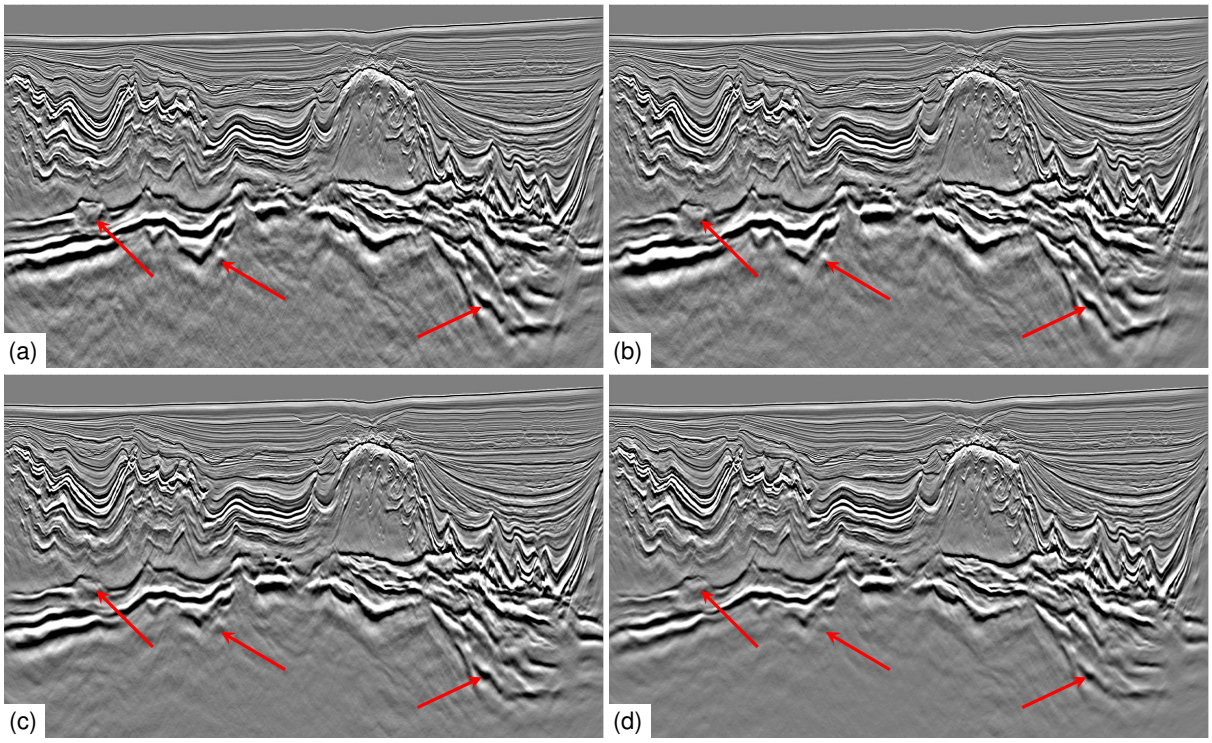

Figure 7: Kirchhoff PSDM stacks for (a) production model and the FWI-derived models with node grids of (b) 500 m by 500 m, (c) 1 km by 1 km, and (d) 2 km by 2 km.